DISCRETE AND CONTINUOUS
DYNAMICAL SYSTEMS SERIES B
Volume **20**, Number **5**, July **2015**

doi:10.3934/dcdsb.2015.20.1405

pp. **1405–1426**

POLYNOMIAL PRESERVING RECOVERY OF AN OVER-PENALIZED SYMMETRIC INTERIOR PENALTY GALERKIN METHOD FOR ELLIPTIC PROBLEMS

Lunji Song

School of Mathematics and Statistics, and Key Laboratory of Applied Mathematics and Complex Systems in Gansu Province, Lanzhou University
Lanzhou 730000, China

Zhimin Zhang

Beijing Computational Science Research Center
Beijing 100094, China
and
Department of Mathematics, Wayne State University
Detroit, MI 48202, USA

Abstract. A polynomial preserving recovery technique is applied to an over-penalized symmetric interior penalty method. The discontinuous Galerkin solution values are used to recover the gradient and to further construct an a posteriori error estimator in the energy norm. In addition, for uniform triangular meshes and mildly structured meshes satisfying the ϵ-σ condition, the method for the linear element is superconvergent under the regular pattern and under the chevron pattern, while it is superconvergent for the quadratic element under the regular pattern.

1. **Introduction.** A posteriori error estimates based on recovery techniques have become standard in finite element methods and and attracted interests of many researchers from the fields of modern engineering and scientific computation. Two types of error estimates are known as the residual type [3, 5] and the recovery type [20, 22]. The most representative recovery type on error estimates is the Zienkiewicz-Zhu error estimator [23], which is referred to the Superconvergence Patch Recovery (SPR) based on gradient recovery from the gradient of the finite element solution by local discrete least-squares fitting. It is well known that the robustness of the ZZ patch recovery is originated from its superconvergence under structured meshes. Generally speaking, if the recovered quantity better approximates the exact one, then it can be used in building asymptotically exact a posteriori error estimates (see [1]). In another strategy, Naga and Zhang first introduced the Polynomial Preserving Recovery (PPR) by using the fitted solution values to recover the gradient and further to construct a posteriori error estimates in the energy

2010 *Mathematics Subject Classification.* Primary: 65N15, 65N30, 97N50.

Key words and phrases. Symmetric interior penalty Galerkin method, PPR, discrete least-squares fitting, superconvergence, a posteriori error estimator.

The first author of this work was partially supported by the National Natural Sciences Foundation of China (Grants 11101196 and 11471150) and by the Natural Science Foundation of Gansu Province, China (Grant 145RJZA046). And the second author was supported in part by the National Natural Science Foundation of China (Grants 11471031 and 91430216), and the US National Science Foundation (Grant DMS-1419040).

norm. The PPR keeps all known superconvergence properties of the ZZ patch recovery but outperforms the SPR in the cases of quadratic element at edge centers and linear element for the chevron mesh [19]. The PPR even superconverges in mildly structured grids.

While there is an amount of work on theoretical investments for residual type error estimates (see [1, 4, 7] and the references therein) and recovery type error estimates (see [18, 22, 24]) in postprocessing continuous finite element solutions, there have been few theoretical results to postprocess discontinuous Galerkin finite element solutions for structured or unstructured grids in recovery type. We observe that for structured grids, the PPR implemented in discontinuous solutions is able to establish superconvergence order; moreover, when adaptive is used for some mildly structured meshes, locally structure in mesh refinement will improve astonishingly superconvergence results.

Let $\Omega \subset \mathbb{R}^2$ be a bounded polynomial domain. Setting the boundary of the domain $\partial\Omega$ composed by the union of two disjoint sets Γ_D and Γ_N, we denote $\mathbf{n}$ the unit normal vector to each edge of $\partial\Omega$ exterior to the domain. For $f \in L^2(\Omega)$, $g_D \in H^{\frac{1}{2}}(\Gamma_D)$, and $g_N \in L^2(\Gamma_N)$, we consider the following elliptic problem

$$\begin{cases} -\nabla \cdot (\mathbf{K}\nabla u) + \alpha u = f, & \text{in } \Omega, \\ u = g_D, & \text{on } \Gamma_D, \\ \mathbf{K}\nabla u \cdot \mathbf{n} = g_N, & \text{on } \Gamma_N. \end{cases} \tag{1}$$

where α is a nonnegative scalar function satisfying that $\alpha \in L^\infty(\Omega)$, and $\mathbf{K}$ is a 2×2-matrix-valued function $\mathbf{K}(x) = (k_{ij}(x))$ that is symmetric positive definite.

The PPR will be applied into an Over-Penalized Symmetric Interior Penalty Galerkin method (OPSIPG) [16] to realize a gradient recovery. The OPSIPG method has some similar features as the Weakly Over-Penalized Symmetric Interior Penalty method (WOPSIP) presented by Brenner etc. in [6, 7]. A local discrete least-squares fitting can be used to discontinuous function values, while node patches can include all neighbor nodes one more times and best fits discontinuous finite element solutions at nodes in any patch.

Based on the PPR, we can consider a posteriori error estimats as they were shown in [24]. If the recovered gradient superconverges to the exact one, the corresponding a posteriori error estimator is asymptotically exact. This will be testified by our last example in this work.

The purpose of this paper is to propose and analyze superconvergence of the PPR in corporation with the OPSIPG method and testify an a posteriori error estimator. We advocate the PPR based on a DG formulation for two reasons:

(i) flexibility for discontinuous coefficients and singularity problems and hp-adaptivity (locally refined meshes available and different orders of polynomials used for different elements) by using the discontinuous Galerkin formulation (see [2, 6, 10] and the references therein).

(ii) appreciation of the robustness of the PPR based on discontinuous function values and its superconvergence property for gradient recovery. Indeed, the least-squares fitting confirms uniqueness of recovery systems dependent on the numbers of nodes appearing in each patch instead of the times of nodes used.

The plan of this paper is organized as follows. In Section 2, the OPSIPG method is introduced and some known estimates are listed. Moreover, we simplify the diffusion term by a piecewise constant matrix approximating the diffusion matrix,

and bound the difference between an interpolation of the exact solution and numerical solutions in the energy norm. Then we give a detailed description for the polynomial preserving gradient recovery in Section 3, and then show that the PPR recovery is superconvergent and prove asymptotic exactness of the recovery type error estimates in Section 4. At the end of the paper, some numerical examples are provided to practically show that as a postprocessing technique for the OPSIPG method, the PPR recovered gradient superconverges to the exact gradient.

2. **OPSIPG method and some estimates.**

2.1. **OPSIPG method.** Let $\mathcal{T}_h = \{E_k\}_{k=1}^{N_h}$ be a subdivision of Ω, where the element E_k is a triangle and N_h is the total number of the elements. The maximum diameter of all elements is denoted by h. We assume that for each element E, $\mathbf{K}$ is bounded below and above uniformly; i.e., there exist two positive constants K_1^E and K_2^E independent of x and $\mathbf{z}$ such that

$$K_1^E \mathbf{z}\cdot\mathbf{z} \le \mathbf{K}(x)\mathbf{z}\cdot\mathbf{z} \le K_2^E \mathbf{z}\cdot\mathbf{z}, \quad \forall\, x \in \bar{E},\, \forall\, \mathbf{z} \in \mathbb{R}^2. \tag{2}$$

We also set K_1 (resp. K_2) the minimum (resp. maximum) of K_1^E (resp. K_2^E) over all elements E in the triangulation $\mathcal{T}_h$. Let Γ_{int} be the set of interior edges of $\mathcal{T}_h$. For each edge e shared by two elements, we associate with e a unit normal vector $\mathbf{n}_e$. If edge e is on the boundary $\partial\Omega$, $\mathbf{n}_e$ is taken to be the unit outward normal vector to $\partial\Omega$.

Along this article, we use notation for Sobolev spaces $W^{k,p}(\varpi)$, $1 \le p \le \infty$, with norm $\|\cdot\|_{k,p,\varpi}$ and semi-norm $|\cdot|_{k,p,\varpi}$, for a polygonal Lipschitz domain ϖ. When $p = 2$, we write $W^{k,2}(\varpi) = H^k(\varpi)$ and omit writing indexes p or ϖ whenever $p = 2$ or $\varpi = \Omega$, respectively. By default, $H^0(\varpi)$ denotes $L^2(\varpi)$ with the L^2 inner product $(\cdot,\cdot)$ and the standard L^2-norm $\|\cdot\|_{L^2(\varpi)}$ over the domain ϖ.

Problem (1) has a unique solution in $H^1(\Omega)$ if $|\Gamma_D| > 0$ or if $\alpha \neq 0$, where $|\Gamma_D|$ denotes the measure of Γ_D. When $\partial\Omega = \Gamma_N$ and $\alpha = 0$, problem (1) has a solution in $H^1(\Omega)$ unique up to an additive constant, provided the condition $\int_\Omega f + \int_{\partial\Gamma} g_N = 0$ holds (see [11]).

We now define the broken Sobolev space for any real number s:

$$H^s(\mathcal{T}_h) = \left\{ v \in L^2(\Omega) : \forall\, E \in \mathcal{T}_h,\ v|_E \in H^s(E) \right\},$$

which is equipped with the broken space norm:

$$|||v|||_s := |||v|||_{H^s(\mathcal{T}_h)} = \Big(\sum_{E\in\mathcal{T}_h} \|v\|_{s,E}^2 \Big)^{1/2}.$$

We also introduce a discontinuous finite element subspace

$$\mathcal{D}_r(\mathcal{T}_h) = \left\{ v \in L^2(\Omega) : \forall\, E \in \mathcal{T}_h,\ v|_E \in \mathbb{P}_r(E),\ r \ge 1 \right\}, \tag{3}$$

where $\mathbb{P}_r(E)$ denotes the set on E of all polynomials of (total) degree at most r on E. If an edge $e \in \Gamma_{int}$ is shared by two elements E_e^1 and E_e^2, we assign the unit vector $\mathbf{n}_e$ normal to e which points from E_e^1 to E_e^2, and then define the average and the jump for $v \in H^s(\mathcal{T}_h)$ with $s > \frac{1}{2}$ on an edge e shared by two elements E_e^1 and E_e^2:

$$\{v\} := \frac{1}{2}(v|_{E_e^1} + v|_{E_e^2})|_e, \quad [v] := (v|_{E_e^1} - v|_{E_e^2})|_e, \quad \forall\, e = \partial E_e^1 \cap \partial E_e^2.$$

If an edge $e \in E_e$ is on the boundary $\partial\Omega$, we associate the unit normal vector $\mathbf{n}_e = \mathbf{n}$ exterior to Ω, and set

$$\{v\} := (v|_{E_e})|_e, \quad [v] := (v|_{E_e})|_e, \quad \forall\, e = \partial E_e \cap \partial\Omega.$$

Let a real number s satisfy $s \geq 2$. Under the above assumptions on $\mathbf{K}$ and α, we consider the symmetric bilinear form $A : H^s(\mathcal{T}_h) \times H^s(\mathcal{T}_h) \mapsto \mathbb{R}$:

$$\begin{aligned} A(w,v) = &\sum_{T\in\mathcal{T}_h} \int_T (\mathbf{K}\nabla w \cdot \nabla v + \alpha w v)dx - \sum_{e\in\Gamma_{int}\cup\Gamma_D} \int_e \{\mathbf{K}\nabla w \cdot \mathbf{n}_e\}[v]ds \\ &- \sum_{e\in\Gamma_{int}\cup\Gamma_D} \int_e \{\mathbf{K}\nabla v \cdot \mathbf{n}_e\}[w]ds + J_0^{\sigma,\beta}(w,v), \end{aligned} \tag{4}$$

where the penalty term is defined by

$$J_0^{\sigma,\beta}(w,v) = \sum_{e\in\Gamma_{int}\cup\Gamma_D} \frac{\sigma_e}{|e|^\beta} \int_e [w][v]ds.$$

Here the penalty parameter σ_e takes the positive constant value on the edge e and is bounded below by σ_1, above by σ_2 and the power β is a positive number to be specified later. In general, the power $\beta = 1$ is taken in nonsymmetric and symmetric methods in many applications. Especially, we say that the DG method is over-penalized if $\beta > 1$. σ_e is referred to as a superpenalty parameter.

Define a linear form

$$L(v) = \int_\Omega fv dx - \sum_{e\in\Gamma_D} \int_e \Big(\mathbf{K}\nabla v \cdot \mathbf{n}_e - \frac{\sigma_e}{|e|^\beta} v\Big) g_D ds + \sum_{e\in\Gamma_N} \int_e v g_N ds. \tag{5}$$

The variational formulation of (1) based on the symmetric interior penalty method is:

Find $u_h \in \mathcal{D}_r(\mathcal{T}_h)$ such that

$$A(u_h, v) = L(v), \quad \forall\, v \in \mathcal{D}_r(\mathcal{T}_h). \tag{6}$$

Define the energy norm on $\mathcal{D}_r(\mathcal{T}_h)$:

$$\|v\|_{\mathcal{E}} = \Big(\sum_{T\in\mathcal{T}_h} \int_T (\mathbf{K}\nabla v \cdot \nabla v + \alpha v^2) + J_0^{\sigma,\beta}(v,v) \Big)^{1/2}.$$

It is well known that the symmetric method is consistent with the model problem (see [2, 17, 16]).

Lemma 2.1. *The exact solution of (1) satisfies the discrete variational problem (6) in two dimensions.*

Next, the following lemmas present the sharp estimate on penalty parameters and an optimal continuity coefficient, which are parallel to the proof of Theorem 9 in [10] contributed by Epshteyn and Rivière. We omit the proofs.

Lemma 2.2. *Define by $\epsilon := (\epsilon^E)_{E\in\mathcal{T}_h}$ a vector of positive components such that ϵ^E is associated to the triangle E (with edges e_1, e_2 and e_3) in $\mathcal{T}_h$. Assume that the bound of the power $\beta \geq 1$ holds. Then, there exists an optimal penalty σ_e^* that depends on r and β such that if $\sigma_e > \sigma_e^*$ we have*

$$A(v,v) \geq C^* \|v\|_{\mathcal{E}}^2, \quad \forall\, v \in \mathcal{D}_r(\mathcal{T}_h), \tag{7}$$

where $C^* = \min\Big\{ \min_{E\in\mathcal{T}_h}(1-\epsilon^E), \min_{e\in\Gamma_{int}\cup\Gamma_D}\Big(1-\frac{\sigma_e^*}{\sigma_e}\Big)\Big\}$. *In detail, for any edge* e*(such as* e_3*)* $\in\Gamma_{int}$ *shared by elements* E_e^1 *and* E_e^2*, the value of the penalty* σ_e^* *was determined exactly by (see* [10]*)*

$$\sigma_e^* = \Big(\frac{3(K_2^E)^2}{2K_1^E\epsilon^E}r(r+1)\cot^\beta\theta^E\Big|_{E=E_e^1} + \frac{3(K_2^E)^2}{2K_1^E\epsilon^E}r(r+1)\cot^\beta\theta^E\Big|_{E=E_e^2}\Big)C_{\beta,e},$$

where θ^E *is the smallest angle in a triangle* E *and* $C_{\beta,e} = (|e_1|+|e_2|)^{\beta-1}$. *Especially, for any edge* $e(:=e_3)\in\Gamma_D\cap\partial E_e$*, it becomes*

$$\sigma_e^* = \frac{6(K_2^E)^2}{2K_1^E\epsilon^E}r(r+1)\cot^\beta\theta^E\Big|_{E=E_e} C_{\beta,e}.$$

Lemma 2.3. *Assume that the bound of the power* $\beta\geq 1$ *holds. Then, there exists an optimal constant* $\bar{C}$ *that depends on* r *and* β *such that*

$$A(w,v)\leq \bar{C}\|w\|_{\mathcal{E}}\|v\|_{\mathcal{E}},\quad \forall\, w,v\in\mathcal{D}_r(\mathcal{T}_h), \tag{8}$$

where $\bar{C} = \max\Big\{\max_{E\in\mathcal{T}_h}(1+\epsilon^E), \max_{e\in\Gamma_{int}\cup\Gamma_D}\Big(1+\frac{\sigma_e^*}{\sigma_e}\Big)\Big\}$.

Let θ denote the smallest angle over all triangles in the subdivision. Assume that the same polynomial degree r is used everywhere. Estimates of the threshold values for the penalty parameters are obtained by taking $\epsilon^E = 1$ as follows

$$\sigma^*_{threshold} = \frac{3K_2^2}{K_1}r(r+1)\cot^\beta\theta C_{\beta,e},\quad \forall\, e\in\Gamma_{int}, \tag{9}$$

$$\sigma^*_{threshold} = \frac{6K_2^2}{K_1}r(r+1)\cot^\beta\theta C_{\beta,e},\quad \forall\, e\in\Gamma_D. \tag{10}$$

Note that the threshold values in [10] are recovered by taking $\beta = 1$ for the estimates above.

A priori energy error estimates for the problem with mixed boundary conditions were derived in [16]. In fact, it is also an error estimate for the OPSIPG method.

Definition 2.4. *Condition A*: The approximation u_I of the exact solution u can be chosen to be continuous. In addition, either the Dirichlet data g_D is a continuous piecewise polynomial of degree k, or the whole boundary is a Neumann boundary ($\partial\Omega = \Gamma_N$).

Theorem 2.5. *Under the above assumptions on the data (including* $\mathbf{K}$*), and if the solution* u *of problem* (1) *satisfies* $u\in H^s(\mathcal{T}_h)$*. Then, there exist a constant* C *independent of* h *such that*

$$\|u-u_h\|_{L^2(\Omega)}\leq Ch^{\min(r+1,s)}|||u|||_{H^s(\mathcal{T}_h)}, \tag{11}$$

and

$$\|u-u_h\|_{\mathcal{E}}\leq Ch^{\min(r+1,s)-1}|||u|||_{H^s(\mathcal{T}_h)}. \tag{12}$$

The estimates are valid if Condition A holds true and if $\beta\geq 1$.

The proof of this theorem for a triangulation over the domain Ω is given in [16]. In the remainder of this work, $A\lesssim B$ is used instead of $A\leq CB$, for some positive generic constant C independent of h, r and s.

2.2. **Simplification of the diffusion term.** Take K_0 as a piecewise constant function such that on each element $E \in \mathcal{T}_h$,

$$K_0|_E = \frac{1}{|E|}\int_E \mathbf{K}(x)dx.$$

Now we define the following auxiliary terms

$$\begin{aligned} a(u,v) &= \int_\Omega \mathbf{K}\nabla u \cdot \nabla v dx, \\ a^E(u,v) &= \int_E K_0 \nabla u \cdot \nabla v dx, \quad E \in \mathcal{T}_h, \\ e_h &= u - u_h. \end{aligned}$$

Assume that $k_{ij} \in C^{0,\kappa}(\Omega)$, it is straightforward to show that

$$\Big| a(e_h, v) - \sum_{E\in\mathcal{T}_h} a^E(e_h, v)\Big| \le Ch^\kappa |e_h|_{1,\Omega}|v|_{1,\Omega}, \quad \kappa > 0. \tag{13}$$

Therefore, we may shift our analysis to the terms $a^E(e_h, v)$. Since $\mathbf{K}(x)$ is symmetric and positive define, so is $K_0|_E$. Then there exists an orthogonal matrix Q_E such that

$$K_0|_E = Q_E^T D_E Q_E$$

with the positive eigenvalue matrix $D_E = diag(d_1^E, d_2^E)$. By changing of variable $x = Q_E z$, we have

$$a^E(e_h, v) = \int_{E_z} D_E \nabla_z e_h \cdot \nabla_z v \det Q_E dz, \tag{14}$$

where $\nabla_z = Q_E \nabla_x$, $\det Q_E = \pm 1$, and E_z is obtained by rotating E. Therefore, we may mainly concentrate on the second order form

$$\int_E D_E \nabla e_h \cdot \nabla v dx = \int_E \Big(d_1^E \frac{\partial e_h}{\partial x_1}\frac{\partial v}{\partial x_1} + d_2^E \frac{\partial e_h}{\partial x_2}\frac{\partial v}{\partial x_2}\Big) dx$$

with $d_i^E > 0$ (i=1,2) and estimate the approximate bilinear term

$$\begin{aligned} A^s(e_h, v) = &\sum_{T\in\mathcal{T}_h}\int_T (D_T \nabla e_h \cdot \nabla v + \alpha e_h v)dx - \sum_{e\in\Gamma_{int}\cup\Gamma_D}\int_e \{\mathbf{K}\nabla e_h \cdot \mathbf{n}_e\}[v]ds \\ &- \sum_{e\in\Gamma_{int}\cup\Gamma_D}\int_e \{\mathbf{K}\nabla v \cdot \mathbf{n}_e\}[e_h]ds + J_0^{\sigma,\beta}(e_h, v), \end{aligned} \tag{15}$$

By consistency (see Lemma 2.1), the error satisfies the orthogonality equation

$$A(e_h, v) = 0, \quad \forall\, v \in \mathcal{D}_r(\mathcal{T}_h).$$

For a continuous interpolation u_I of u, denoting $e_I = u - u_I$, adding and subtracting u_I in each term yields

$$A(e_I, v) = A(u_h - u_I, v), \quad \forall\, v \in \mathcal{D}_r(\mathcal{T}_h). \tag{16}$$

Using (7) with taking $v = u_h - u_I \in \mathcal{D}_r(\mathcal{T}_h)$, we have

$$\|u_h - u_I\|_{\mathcal{E}} \le \frac{A(u_h - u_I, v)}{C^*\|v\|_{\mathcal{E}}} = \frac{A(e_I, v)}{C^*\|v\|_{\mathcal{E}}}, \quad \forall\, v \in \mathcal{D}_r(\mathcal{T}_h). \tag{17}$$

Note that the bilinear term $A^s(e_I, v)$ has a little of difference from $A(e_I, v)$ about the matrix-valued function $\mathbf{K}$ on each element. Therefore, it is straightforward to show that

$$\|A(e_I, v) - A^s(e_I, v)\| \leq \max\{K_1, \|\alpha\|_\infty\} h \|e_I\|_{1,\Omega} \|v\|_{\mathcal{E}}, \tag{18}$$

which means that one can shift the analysis to the approximate term $A^s(e_I, v)$. We consider

$$\begin{aligned} &A^s(e_I, v) \\ &= \sum_{T\in\mathcal{T}_h} \int_T K_0 \nabla e_I \cdot \nabla v dx + \sum_{T\in\mathcal{T}_h} \int_T \alpha e_I v dx - \sum_{e\in\Gamma_{int}\cup\Gamma_D} \int_e \{\mathbf{K}\nabla e_I \cdot \mathbf{n}_e\}[v] ds \\ &:= T_1 + T_2 + T_3. \end{aligned} \tag{19}$$

2.3. **The superconvergence of $\|u_I - u_h\|_{\mathcal{E}}$.** To estimate $\|u_I - u_h\|_{\mathcal{E}}$ in (17), we need to bound the three terms in (19).

To bound term T_1, we can use the known results in [21] (see (2.10) and (2.12) therein). Let $S_{h,r}$ be a C^0 polynomial finite element space of degree r ($r = 1$ or 2) over $\mathcal{T}_h$.

Definition 2.6. $\mathcal{T}_h$ satisfies *Condition* (ϵ, σ) if $\mathcal{T}_h$ can be separated into two parts

$$\mathcal{T}_h = \mathcal{T}_{0,h} \cup \mathcal{T}_{1,h}, \qquad \bigcup_{E\in\mathcal{T}_{i,h}} \bar{E} = \bar{\Omega}_{i,h}, \quad \bar{\Omega} = \bar{\Omega}_{0,h} \cup \bar{\Omega}_{1,h},$$

such that the following conditions exist:

1. Any two triangles that share a common edge in $\mathcal{T}_{0,h}$ form a convex quadrilateral which is an ϵ-perturbation from a parallelogram.

2. $\Omega_{1,h}$ has a small measure: $|\Omega_{1,h}| = O(h^\sigma)$, $\sigma > 0$.

Notice that the test function v in the term T_1 is not in $S_{h,r}$, but in the broken finite element space $\mathcal{D}_r(\mathcal{T}_h)$. We recall the so-called Oswald interpolation operator O_s, which has been analyzed in [8, 14]. There exists a constant $C_r := r^{-\frac{1}{2}}$ dependent only on r, such that, for all $T \in \mathcal{T}_h$, the following estimate holds

$$\|v_h - O_s v_h\|_{L^2(T)} \lesssim C_r h_T^{\frac{1}{2}} \sum_{e\in\Gamma_{int}\cap T} \|[v_h]\|_{L^2(e)}, \qquad \forall\, v_h \in \mathcal{D}_r(\mathcal{T}_h). \tag{20}$$

Denote by Q_h the L^2 projection onto $S_{h,r}$ such that

$$(w_h, Q_h v_h) = (w_h, v_h), \qquad w_h \in S_{h,r},\ v_h \in \mathcal{D}_r(\mathcal{T}_h).$$

By the fact that $\|v_h - Q_h v_h\|_{L^2(\mathcal{T}_h)} \leq \|v_h - O_s v_h\|_{L^2(\mathcal{T}_h)}$, it holds from (20)

$$\|v_h - Q_h v_h\|_{L^2(\mathcal{T}_h)} \lesssim C_r h^{\frac{1}{2}} \Big(\sum_{e\in\Gamma_{int}} \|[v_h]\|^2_{L^2(e)} \Big)^{\frac{1}{2}}, \tag{21}$$

and by inverse inequality,

$$\|\nabla(v_h - Q_h v_h)\|_{L^2(\mathcal{T}_h)} \lesssim r^2 C_r h^{-\frac{1}{2}} \Big(\sum_{e\in\Gamma_{int}} \|[v_h]\|^2_{L^2(e)} \Big)^{\frac{1}{2}}, \tag{22}$$

which means that we can prove the following lemmas 2.7-2.8 by using the decomposition

$$\nabla v = \nabla(Q_h v) + \nabla(v - Q_h v),$$

By utilizing an integral identity for linear element on triangular elements, Zhang generalized the superconvergence result between the finite element solution and the

linear interpolation in [21, Theorem 2.1 and (2.14)], while Huang and Xu proved the superconvergence result between the quadratic finite element solutions and its quadratic interpolation in [12, Theorems 4.2 and 4.3]. Consequently, we can directly apply these superconvergence results into the decomposition above and get the following lemmas 2.7 and 2.8.

Lemma 2.7. *(Linear finite element) Let $u \in H^3(\Omega) \cap W^{2,\infty}(\Omega)$ and $u_I \in \mathcal{D}_1(\mathcal{T}_h)$ be the solution of the model problem and its Lagrange linear finite element interpolation, respectively. Assume that $\mathcal{T}_h$ satisfies Condition (ϵ, σ). Then the error bound*

$$\begin{aligned}&\sum_{T\in\mathcal{T}_h}\int_T K_0\nabla e_I\cdot\nabla v dx\\ &\lesssim \Big(h^{3/2}(\|u\|_{3,\Omega}+\epsilon)+h\epsilon(\|u\|_{2,\Omega_{0,h}}+\epsilon)+\big(h^{\frac{2+\sigma}{2}}+h^{\frac{\beta+1}{2}}\big)|u|_{2,\infty,\Omega}\Big)\|v\|_{\mathcal{E}}.\end{aligned} \tag{23}$$

holds for all $v \in \mathcal{D}_1(\mathcal{T}_h)$. Here $\|u\|^2_{k,\Omega_{0,h}} := \sum_{E\in\mathcal{T}_{0,h}} \|u\|^2_{k,E}$.

Lemma 2.8. *(Quadratic finite element) Let $u \in W^{4,p}(\Omega) \cap W^{3,\infty}(\Omega)$ and $u_I \in \mathcal{D}_2(\mathcal{T}_h)$ be the solution of the model problem and its Lagrange quadratic finite element interpolation, respectively.*
(1) If the triangulation $\mathcal{T}_h$ is uniform, then, for $p, q \geq 1$ with $\frac{1}{p}+\frac{1}{q}=1$, we have

$$\sum_{T\in\mathcal{T}_h}\int_T K_0\nabla e_I\cdot\nabla v dx \lesssim h^{4-\alpha}|u|_{4,p,\Omega}|v|'_{2-\alpha,q,\Omega}, \quad v\in S_{h,r}.$$

Here $|v|'_{2-\alpha,q,\Omega} = \Big(\sum_{E\in\mathcal{T}_h}|v|^q_{2-\alpha,q,E}\Big)^{\frac{1}{q}}$ and K_0 is independent of T. The superconvergence estimate can be obtained by taking $\alpha = 1$. Especially, $|v|'_{2-\alpha,q,\Omega} = |v|_{1,\Omega}$, when $\alpha = 1$ and $p = q = 2$. Therefore, it holds

$$\sum_{T\in\mathcal{T}_h}\int_T K_0\nabla e_I\cdot\nabla v dx \lesssim h^3|u|_{4,\Omega}\|v\|_{\mathcal{E}}, \quad v\in\mathcal{D}_2(\mathcal{T}_h). \tag{24}$$

(2) If the triangulation $\mathcal{T}_h$ is strongly regular so that any two adjacent triangles form an $\mathcal{O}(h^2)$ approximate parallelogram, then

$$\sum_{T\in\mathcal{T}_h}\int_T K_0\nabla e_I\cdot\nabla v dx \lesssim h^{4-\alpha}|u|_{4,p,\Omega}|v|'_{2-\alpha,q,\Omega}, \quad v\in S_{h,r}. \tag{25}$$

The superconvergence estimate can be obtained by taking $\alpha = 1$. Especially, $|v|'_{2-\alpha,q,\Omega} = |v|_{1,\Omega}$, when $\alpha = 1$ and $p = q = 2$. Therefore, it holds

$$\sum_{T\in\mathcal{T}_h}\int_T K_0\nabla e_I\cdot\nabla v dx \lesssim h^3|u|_{4,\Omega}\|v\|_{\mathcal{E}}, \quad v\in\mathcal{D}_2(\mathcal{T}_h). \tag{26}$$

(3) Assume that $\mathcal{T}_h$ satisfies Condition (ϵ, σ). Then the error bound holds

$$\begin{aligned}&\sum_{T\in\mathcal{T}_h}\int_T K_0\nabla e_I\cdot\nabla v dx\\ &\lesssim \Big(h^{5/2}(\|u\|_{4,\Omega_{0,h}}+\epsilon)+h^2\epsilon(\|u\|_{3,\Omega}+\epsilon)+\big(h^{\frac{4+\sigma}{2}}+h^{\frac{\beta+3}{2}}\big)|u|_{3,\infty,\Omega}\Big)\|v\|_{\mathcal{E}}.\end{aligned} \tag{27}$$

Next, for $s \geq r+1$, by Cauchy-Schwarz inequality and the standard approximation theory, we have

$$\begin{aligned} |T_2| &= \Big| \int_\Omega \alpha e_I v dx \Big| \\ &\lesssim \Big| \int_\Omega (\alpha^{1/2} e_I)(\alpha^{1/2} v) dx \Big| \lesssim h^{r+1} |u|_{r+1,\Omega} \Big(\sum_{T \in \mathcal{T}_h} \int_T |\alpha v^2| dx \Big)^{1/2}. \end{aligned} \tag{28}$$

Using the trace inequality and Cauchy-Schwarz inequality, we bound the term T_3

$$\begin{aligned} |T_3| &\leq \Big(\frac{K_1}{\sigma^*} \sum_{e \in \Gamma_{int}} |e|^\beta \|\nabla e_I\|_e^2 \Big)^{\frac{1}{2}} J_0^{\sigma,\beta}(v,v)^{\frac{1}{2}} \\ &\leq \Big(\frac{K_1}{\sigma^*} \sum_{E \in \mathcal{T}_h} |e|^\beta h_e^{-1} \|\nabla e_I\|_E^2 \Big)^{\frac{1}{2}} J_0^{\sigma,\beta}(v,v)^{\frac{1}{2}} \\ &\leq \Big(\frac{K_1}{\sigma^*} \sum_{E \in \mathcal{T}_h} |e|^\beta h^{2r-1} \|u\|_{r+1,E}^2 \Big)^{\frac{1}{2}} J_0^{\sigma,\beta}(v,v)^{\frac{1}{2}} \\ &\lesssim h^{r+\frac{\beta-1}{2}} \|u\|_{r+1,\Omega} J_0^{\sigma,\beta}(v,v)^{\frac{1}{2}}. \end{aligned} \tag{29}$$

Based on the definition of the broken energy norm $\|\cdot\|_{\mathcal{T}_h}$, and from Lemmas 2.7 and 2.8, (28)-(29), we derive the bound of $|A^s(e_I, v)|$

$$|A^s(e_I, v)| \lesssim \Big(\mathcal{F}_h + h^{r+1} + h^{r+\frac{\beta-1}{2}} \Big) \|v\|_{\mathcal{E}}, \tag{30}$$

where the term $\mathcal{F}_h$ has the following forms in the term T_1:
(1) for piecewise linear finite element in $\mathcal{D}_1(\mathcal{T}_h)$,

$$\mathcal{F}_h = h^{3/2}(\|u\|_{3,\Omega} + \epsilon) + h\epsilon(\|u\|_{2,\Omega_{0,h}} + \epsilon) + \big(h^{\frac{2+\sigma}{2}} + h^{\frac{\beta+1}{2}}\big)|u|_{2,\infty,\Omega}. \tag{31}$$

(2) for piecewise quadratic finite element in $\mathcal{D}_2(\mathcal{T}_h)$,

$$\mathcal{F}_h = \begin{cases} h^3 \|u\|_{4,\Omega}, & \text{if the triangulation } \mathcal{T}_h \text{ is uniform or strongly regular,} \\ h^{5/2}(\|u\|_{4,\Omega_{0,h}} + \epsilon) + h^2\epsilon(\|u\|_{3,\Omega} + \epsilon) + \big(h^{\frac{4+\sigma}{2}} + h^{\frac{\beta+3}{2}}\big)|u|_{3,\infty,\Omega}, & \text{if} \\ \mathcal{T}_h \text{ satisfies } \textit{Condition } (\epsilon, \sigma). \end{cases} \tag{32}$$

Then from (17)-(18) and (19), we get the following superconvergence estimates for $\|u_I - u_h\|_{\mathcal{E}}$ in different grids.

Theorem 2.9. *Let $u \in H^{r+2}(\Omega) \cap W^{r+1,\infty}(\Omega)$ and $u_h \in \mathcal{D}_r(\mathcal{T}_h)$ be the solution of the model problem (1) and its discontinuous Galerkin finite element approximation in (6), respectively. u_I is assumed to be an r-th order Lagrangian interpolation of u.*

If $r = 1$, and $\mathcal{T}_h$ satisfies Condition (ϵ, σ), then

$$\begin{aligned} &\|u_I - u_h\|_{\mathcal{E}} \\ &\lesssim \Big(h \max\{h^{1/2}, \epsilon, h^{\sigma/2}\} + h^2 + h^{1+\frac{\beta-1}{2}} \Big) (\|u\|_{3,\Omega} + \|u\|_{2,\Omega} + |u|_{2,\infty,\Omega}). \end{aligned} \tag{33}$$

If $r = 2$, and $\mathcal{T}_h$ is uniform or strongly regular, then

$$\|u_I - u_h\|_{\mathcal{E}} \lesssim \Big(h^3 + h^{2+\frac{\beta-1}{2}} \Big) (\|u\|_{4,\Omega} + \|u\|_{3,\Omega}). \tag{34}$$

If $r = 2$, and $\mathcal{T}_h$ satisfies Condition (ϵ, σ), then

$$\|u_I - u_h\|_{\mathcal{E}} \lesssim \left(h^2 \max\{h^{1/2}, \epsilon, h^{\sigma/2}\} + h^3 + h^{2+\frac{\beta-1}{2}}\right)(\|u\|_{4,\Omega} + \|u\|_{3,\Omega} + |u|_{3,\infty,\Omega}). \tag{35}$$

Remark 1. It is observed that Theorem 2.9 shows superconvergence results under the condition $\beta > 1$, which means the symmetric interior penalty method as an overpenalized one. In the case for general grids, most pairs of triangles form an approximate parallelogram although the entire grid is not strongly regular. Here the condition on ϵ is weakened, even not to require every two adjacent triangles form an $O(h^{1+\alpha})$ parallelogram as discussed in [18, 24].

3. **Polynomial preserving gradient recovery.** Following [19, 21], we introduce a gradient recovery operator $G_h : \mathcal{D}_r(\mathcal{T}_h) \to S_{h,r} \times S_{h,r}$, where $S_{h,r}$ is a C^0 polynomial finite element space of degree r ($r = 1$ or 2) over the triangulation $\mathcal{T}_h$. For any r-th order element, all we need is to define $G_h u_h$ at each node z_i of the triangulation $\mathcal{T}_h$:

$$G_h u_h(z_i) = \sum_j \mathbf{C}_{ij} u_h(z_{ij}), \quad \sum_j \mathbf{C}_{ij} = 0,$$

where $\mathbf{C}_{ij}$ are coefficients of some finite difference schemes. In some special situations, we refer to [20] for the choices of $\mathbf{C}_{ij}$. It means that the recovered gradient at z_i is a linear combination of some nearby nodal values of the discontinuous finite element solution.

First, we present definition of the PPR for discontinuous approximations. Let $z \in \mathcal{N}_h$ be a mesh vertex and let $\mathcal{T}_{h,z}$ denote a patch of mesh elements around z. Set $p_z \in \mathbb{P}_{r+1}$ be the polynomial that best fits discontinuous solutions u_h at the mesh nodes in $\mathcal{T}_{h,z}$ in the local discrete least-squares sense:

$$\sum_{z_i \in \mathcal{N}_h \cap \mathcal{T}_{h,z}} |(u_h - p_z)(z_i)|^2 = \min_{p \in \mathbb{P}_{r+1}(\mathcal{T}_{h,z})} \sum_{z_i \in \mathcal{N}_h \cap \mathcal{T}_{h,z}} |(u_h - p)(z_i))|^2. \tag{36}$$

We call p_z the least-squares polynomial approximation (LSPA) of u_h at z. Then it is well defined by

$$(G_h u_h)(z) \triangleq \nabla p_z(z).$$

We denote by $N(\mathcal{T}_{h,z})$ the number of mesh nodes in the patch $\mathcal{T}_{h,z}$. For an internal mesh vertex z and an order r, there are $N(\mathcal{T}_{h,z})$ ($\geq m := \frac{(r+2)(r+3)}{2}$) nodes required in an element patch $\mathcal{T}_{h,z}$ including the mesh vertex z_i. To fit a polynomial of degree $r+1$, in the least-squares sense, we select nodes distributed around z on the circle $B_h(z) = \{x \in \mathcal{T}_h : |x - z| \leq h\}$. If the number of nodes (including z) is less than m, we search further and select nodes in a larger circular domain $B_{2h}(z)$, repeating this process until more than or identical to m nodes are found. Then the patch $\mathcal{T}_{h,z}$ is well defined and must have at least m nodes distributed around z in a way that leads to a unique p_z. Next, to define $\mathcal{T}_{h,z}$ at a boundary mesh vertex z, we set

$$\mathcal{T}_{h,z} \triangleq \mathcal{T}_{h,z_0} \cup \mathcal{L}_{z,n_0}, \tag{37}$$

where z_0 is the closest internal vertex to z and $\mathcal{L}_{z,n_0}$ is the union of mesh elements in the first $n_0 \in \mathbb{Z}^+$ layers around z including the internal mesh vertex z_0. This definition ensures the uniqueness of p_z as shown in Lemma 3.6 of [13].

Let h_z be the length of the longest edge attached to z. Taking the local coordinates (x, y) with z as the origin, the fitting polynomial is

$$p_{r+1}(x, y; z) = \mathbf{P}^T\mathbf{a} = (1, x, y, \cdots, x^{r+1}, x^r y, x^{r-1}y^2, \cdots, y^{r+1})\mathbf{a}$$

with $\mathbf{a}^T = (a_1, a_2, \cdots, a_m)$. With a scaling augment by $h = h_i$, setting

$$\hat{\mathbf{P}}^T = (1, \xi, \eta, \cdots, \xi^{r+1}, \xi^r\eta, \xi^{r-1}\eta^2, \cdots, \eta^{r+1}),$$

the fitting polynomial becomes

$$\hat{p}_{r+1}(\xi, \eta) = \hat{\mathbf{P}}^T\hat{\mathbf{a}},$$

where $\hat{\mathbf{a}}^T = (a_1, ha_2, ha_3, \cdots, h^{k+1}a_m)$. The coefficient vector $\hat{\mathbf{a}}$ is determined by the linear system

$$A^T A\hat{\mathbf{a}} = A^T\mathbf{b}, \tag{38}$$

where $\mathbf{b}^T = (u_h(z_{i1}), u_h(z_{i2}), \cdots, u_h(z_{in}))$ and

$$A = \begin{pmatrix} 1 & \xi_1 & \eta_1 & \cdots & \eta_1^{r+1} \\ 1 & \xi_2 & \eta_2 & \cdots & \eta_2^{r+1} \\ \vdots & \vdots & \vdots & \vdots & \vdots \\ 1 & \xi_n & \eta_n & \cdots & \eta_n^{r+1} \end{pmatrix}.$$

The uniqueness condition for the linear system (38) is $\mathrm{Rank}(A) = m$, so it holds when $n \le m$ and grid points are reasonably distributed.

In order to demonstrate the difference between the present DG PPR and the classical PPR method, we shall discuss two examples in detail on uniform meshes.

Example 1. Linear element on uniform triangular mesh. First, we consider the regular pattern in Figure 1. We fit a quadratic polynomial in (ξ, η) coordinates

$$\hat{p}_2(\xi, \eta) = (1, \xi, \eta, \xi^2, \xi\eta, \eta^2)(\hat{a}_1, \cdots, \hat{a}_6)^T$$

in the least-squares with respect to the 18 nodal values

$$\boldsymbol{\xi} = (0, 0, 0, 0, 0, 0, 1, 1, 0, 0, -1, -1, -1, -1, 0, 0, 1, 1)^T,$$
$$\boldsymbol{\eta} = (0, 0, 0, 0, 0, 0, 0, 0, 1, 1, 1, 1, 0, 0, -1, -1, -1, -1)^T.$$

Denote $\boldsymbol{e} = (1, 1, 1, 1, 1, 1, 1, 1, 1, 1, 1, 1, 1, 1, 1, 1, 1, 1)^T$ and set

$$A = (\mathbf{e}, \boldsymbol{\xi}, \boldsymbol{\eta}, \boldsymbol{\xi}^2, \boldsymbol{\xi\eta}, \boldsymbol{\eta}^2)$$

with $\boldsymbol{\xi}^2 = (\xi_1^2, \xi_2^2, \cdots, \xi_{18}^2)^T$, and $\boldsymbol{\xi\eta}$, $\boldsymbol{\eta}^2$ defined accordingly. By direct calculation, we get $\hat{\mathbf{a}}$ from the formulation (38). For simplicity, we let $\mathbf{b}^T = (u_1, u_2, \cdots, u_{18})$ instead of using the discontinuous finite element solution u_h. Notice that $\hat{\mathbf{a}} =$

$(a_1, ha_2, ha_3, h^2a_4, h^2a_5, h^2a_6)$, then we get

$$
\begin{aligned}
p_2(x,y;z) &= \frac{1}{6}(u_1+u_2+u_3+u_4+u_5+u_6)\\
&+\frac{1}{12h}[2(u_7+u_8)+u_9+u_{10}-u_{11}-u_{12}-2(u_{13}+u_{14})-u_{15}-u_{16}+u_{17}+u_{18}]x\\
&+\frac{1}{12h}[u_7+u_8+2(u_9+u_{10})+u_{11}+u_{12}-u_{13}-u_{14}-2(u_{15}+u_{16})-u_{17}-u_{18}]y\\
&+\frac{1}{12h^2}[-2(u_1+u_2+u_3+u_4+u_5+u_6)+3(u_7+u_8+u_{13}+u_{14})]x^2\\
&+\frac{1}{12h^2}[-2(u_1+u_2+u_3+u_4+u_5+u_6)\\
&\qquad +3(u_7+u_8+u_9+u_{10}-u_{11}-u_{12}+u_{13}+u_{14}+u_{15}+u_{16}-u_{17}-u_{18})]xy\\
&+\frac{1}{12h^2}[-2(u_1+u_2+u_3+u_4+u_5+u_6)+u_9+u_{10}+u_{15}+u_{16}]y^2.
\end{aligned}
$$

It is observed that

$$
\begin{aligned}
&\frac{\partial p_2}{\partial x}(x,y;z)\\
&=\frac{1}{12h}[2(u_7+u_8)+u_9+u_{10}-u_{11}-u_{12}-2(u_{13}+u_{14})-u_{15}-u_{16}+u_{17}+u_{18}]\\
&\quad+\frac{1}{6h^2}[-2(u_1+u_2+u_3+u_4+u_5+u_6)+3(u_7+u_8+u_{13}+u_{14})]x\\
&\quad+\frac{1}{12h^2}[-2(u_1+u_2+u_3+u_4+u_5+u_6)\\
&\qquad +3(u_7+u_8+u_9+u_{10}-u_{11}-u_{12}+u_{13}+u_{14}+u_{15}+u_{16}-u_{17}-u_{18})]y;
\end{aligned}
$$

and

$$
\begin{aligned}
&\frac{\partial p_2}{\partial y}(x,y;z)\\
&=\frac{1}{12h}[u_7+u_8+2(u_9+u_{10})+u_{11}+u_{12}-u_{13}-u_{14}-2(u_{15}+u_{16})-u_{17}-u_{18}]\\
&\quad+\frac{1}{12h^2}[-2(u_1+u_2+u_3+u_4+u_5+u_6)\\
&\qquad +3(u_7+u_8+u_9+u_{10}-u_{11}-u_{12}+u_{13}+u_{14}+u_{15}+u_{16}-u_{17}-u_{18})]x\\
&\quad+\frac{1}{6h^2}[-2(u_1+u_2+u_3+u_4+u_5+u_6)+u_9+u_{10}+u_{15}+u_{16}]y;
\end{aligned}
$$

It is straightforward to verify that the recovered gradients $\frac{\partial p_2}{\partial x}$ and $\frac{\partial p_2}{\partial y}$ have a second order approximation to ∇u by the Taylor expansion. Comparing to the polynomial and derivatives of p_2 in [19], the corresponding results above means an average representation for discontinuous solutions at the same node. In other words, when numerical solution u_h is discontinuous, under the regular pattern, the least-squares fitting polynomial is constructed by the average of numerical solutions at a vertex, which means smoothness of the discontinuous solutions. Choosing $(x,y)=(0,0)$, we obtain the recovered gradient at a vertex (see Figure 1):

$$
G_h u_h = \frac{1}{12h}\begin{pmatrix} 2(u_7+u_8)+u_9+u_{10}-u_{11}-u_{12}-2(u_{13}+u_{14})-u_{15}-u_{16}+u_{17}+u_{18} \\ u_7+u_8+2(u_9+u_{10})+u_{11}+u_{12}-u_{13}-u_{14}-2(u_{15}+u_{16})-u_{17}-u_{18} \end{pmatrix}. \tag{39}
$$

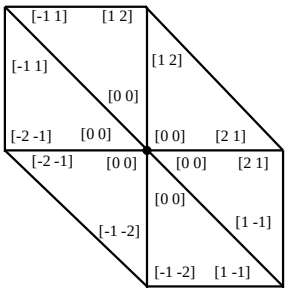

FIGURE 1. Recovery weights for DG solutions in regular mesh: Denominator $12h$.

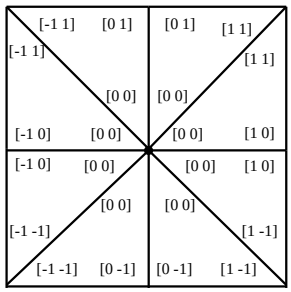

FIGURE 2. Recovery weights for DG solutions in union Jack mesh: Denominator $12h$.

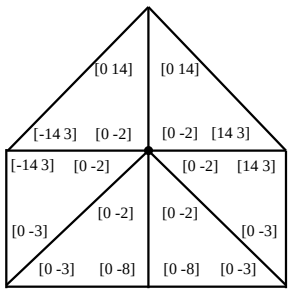

FIGURE 3. Recovery weights for DG solutions in chevron mesh: Denominator $56h$.

Figure 1 shows the weights at the vertex, where each vertex is shared at least by two elements, excerpt for the central vertex shared by six elements. By linear interpolation and computation of $G_h u_h$ in (39) at each vertex, we are able to form a recovered gradient field from numerical solutions. Then we have two means to get the recovered gradient: one is to directly use (39), the other one is to smoothen numerical solution by averaging technique first, and then use the formulae of the recovered gradient given in [19].

For a linear finite element under the Union Jack pattern, following the analogous procedure as the above, we set the 18 nodal values

$$\boldsymbol{\xi} = (0,0,0,0,0,0,0,0,1,1,1,1,0,0,-1,-1,-1,-1,-1,-1,0,0,1,1)^T,$$
$$\boldsymbol{\eta} = (0,0,0,0,0,0,0,0,0,0,1,1,1,1,1,1,0,0,-1,-1,-1,-1,-1,-1)^T.$$

Then an analogous method has been used to get the recovered gradient $G_h u_h$ at a vertex located at the center of a union Jack patch (see Figure 2):

$$\frac{1}{12h}\begin{pmatrix} u_9+u_{10}+u_{11}+u_{12}-u_{15}-u_{16}-u_{17}-u_{18}-u_{19}-u_{20}+u_{23}+u_{24} \\ u_{11}+u_{12}+u_{13}+u_{14}+u_{15}+u_{16}-u_{19}-u_{20}-u_{21}-u_{22}-u_{23}-u_{24} \end{pmatrix}.$$

For the chevron pattern, following the analogous procedure as the above, we set the 18 nodal values

$$\boldsymbol{\xi} = (0,0,0,0,0,0,1,1,0,0,-1,-1,-1,-1,0,0,1,1)^T,$$
$$\boldsymbol{\eta} = (0,0,0,0,0,0,0,0,1,1,0,0,-1,-1,-1,-1,-1,-1)^T.$$

Then, we are able to get the weights of recovered gradient $G_h u_h$ at a vertex located at the center of a chevron patch (see Figure 3). We remark here that if a patch has symmetric elements, then at the same node, the function values have the same weights as indicated in Figures 1-3. Especially, if an origin of a patch is coincide with its centroid, then at any node, its function values share the same weights and the average of the function values at the node has the same weights as conforming finite element solutions shared at this node (see Figures 1-2).

Example 2. Quadratic element on uniform triangular mesh. We need to fit a cubic polynomial

$$\hat{p}_3(\xi,\eta) = (1,\xi,\eta,\xi^2,\xi\eta,\eta^2,\xi^3,\xi^2\eta,\xi\eta^2,\eta^3)(\hat{a}_1,\cdots,\hat{a}_{10})^T,$$

with respect to function values at 36 nodes, which include 18 vertices and 18 edge centers. Following the analogous procedure as in Example 1, we derive the recovered gradient at the vertex (i.e., the center of the mesh patch). Under the regular pattern, it is derived that

$$\begin{aligned}
&\frac{\partial p_2}{\partial x}(x,y;z)\\
&= \frac{1}{96h}\Big(-10(u_7+u_8) - 5(u_9+u_{10}) + 5(u_{11}+u_{12}) + 10(u_{13}+u_{14})\\
&+ 5(u_{15}+u_{16}) - 5(u_{17}+u_{18}) + 38(u_{19}+u_{20}) + 19(u_{21}+u_{22}) - 19(u_{23}+u_{24})\\
&- 38(u_{25}+u_{26}) - 19(u_{27}+u_{28}) + 19(u_{29}+u_{30}) + 14(u_{31}-u_{32}) - 14(u_{34}-u_{36})\Big);
\end{aligned}$$

and

$$\begin{aligned}
&\frac{\partial p_2}{\partial y}(x,y;z)\\
&= \frac{1}{96h}\Big(-5(u_7+u_8) - 10(u_9+u_{10}) - 5(u_{11}+u_{12}) + 5(u_{13}+u_{14})\\
&+ 10(u_{15}+u_{16}) + 5(u_{17}+u_{18}) + 19(u_{19}+u_{20}) + 38(u_{21}+u_{22}) + 19(u_{23}+u_{24})\\
&- 19(u_{25}+u_{26}) - 38(u_{27}+u_{28}) - 19(u_{29}+u_{30}) + 14(u_{31}+u_{32}) - 14(u_{34}+u_{35})\Big).
\end{aligned}$$

Under the chevron pattern, it is derived that

$$\begin{aligned}
&\frac{\partial p_2}{\partial x}(x,y;z)\\
&= \frac{1}{3054h}\Big(3(u_7+u_8) - 3(u_{11}+u_{12}) + 279(u_{13}+u_{14}) - 279(u_{17}+u_{18})\\
&\quad + 729(u_{19}+u_{20}) - 729(u_{23}+u_{24}) - 749(u_{25}+u_{26}) + 749(u_{29}+u_{30})\\
&\quad + 528(u_{31}-u_{32}) - 43(u_{33}-u_{36}) - 588(u_{34}-u_{35})\Big);
\end{aligned}$$

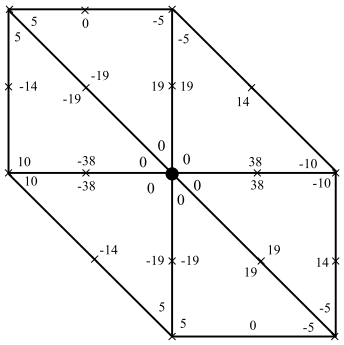

FIGURE 4. *Gradient recovery on x in regular mesh: Denominator $96h$.*

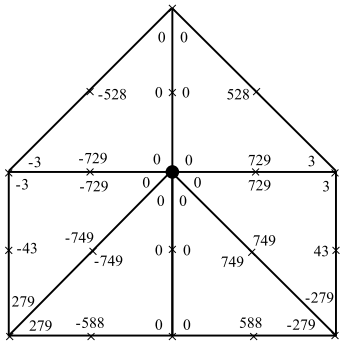

FIGURE 5. *Gradient recovery on x in chevron mesh: Denominator $3054h$.*

and

$$\begin{aligned}
&\frac{\partial p_2}{\partial y}(x,y;z)\\
&= \frac{1}{h}\Big(\frac{259}{5962}(u_1+u_2+u_3+u_4+u_5+u_6)+\frac{69}{4406}(u_7+u_8+u_{11}+u_{12})\\
&\quad -\frac{149}{3369}(u_9+u_{10})+\frac{163}{1886}(u_{13}+u_{14}+u_{17}+u_{18})-\frac{107}{2600}(u_{15}+u_{16})\\
&\quad +\frac{2348}{64335}(u_{19}+u_{20})+\frac{634}{2363}(u_{21}+u_{22})+\frac{2348}{64335}(u_{23}+u_{24})-\frac{639}{3014}(u_{25}+u_{26})\\
&\quad -\frac{1058}{4713}(u_{27}+u_{28})-\frac{639}{3014}(u_{29}+u_{30})+\frac{1943}{8031}(u_{31}+u_{32})-\frac{485}{2778}(u_{33}+u_{36})\\
&\quad -\frac{203}{21925}(u_{34}+u_{35})\Big).
\end{aligned}$$

For simplicity, we shall skip the details and only show the first components of the weights, which means specified finite difference schemes for the x-derivatives from our recovery procedure. Under the regular pattern, Figure 4 shows the first components of the weights at the central vertex on uniform mesh, while Figure 5 shows the counterpart on chevron mesh. The PPR generates finite difference formulas for first order partial derivatives. By the Taylor expansion, the formulas generally have an $(r+1)$-order accuracy, as well as the $(r+2)$-order accuracy attained at a mesh symmetry center of involved nodes in a uniform grid with r being an even number. Especially, these formulas recover the exact derivatives of polynomials in $\mathbb{P}_{r+1}(\Omega)$.

4. **Superconvergence of the PPR and its error estimator.** As mentioned before in many works, the following property holds analogously as in [19].

Polynomial preserving:

$$G_h(p_I)=\nabla p,\quad \forall\, p\in\mathbb{P}_{r+1}(\Omega).$$

This fact is proved in [19]. Consequently, by Bramble-Hilbert Lemma, it has the approximating property

$$\|\nabla u - G_h(u_I)\| \lesssim h^{r+1}\|u\|_{r+2,\Omega},\qquad \forall\, u\in H^{r+2}(\Omega). \tag{40}$$

The reader can be referred to [9] for more details.

Due to the appearance of discontinuity on function values, we cannot directly use the boundedness of the recovery operator G_h like continuous finite element solutions. We need the following boundedness assumption on G_h: When there are no two adjacent angles on an element patch adding up to exceed π, it is assumed that

$$\|G_h v\| \lesssim \|v\|_{\mathcal{E}}, \quad \forall\, v \in \mathcal{D}_r(\mathcal{T}_h). \tag{41}$$

Then the estimate (40) gives

$$\begin{aligned}\|\nabla u - G_h(u_h)\| &\le \|\nabla u - G_h(u_I)\| + \|G_h(u_I) - G_h(u_h)\| \\ &\lesssim h^{r+1}\|u\|_{r+2,\Omega} + \|u_I - u_h\|_{\mathcal{E}},\end{aligned}$$

which infers the following main theorem from Theorem 2.9.

Theorem 4.1. *Assume that $\beta > 1$. Let $u \in H^{r+2}(\Omega) \cap W^{r+1,\infty}(\Omega)$ $(r \ge 1)$ and $u_h \in \mathcal{D}_r(\mathcal{T}_h)$ be the solution of the model problem (1) and its discontinuous Galerkin finite element approximation in (6), respectively. We have the following results:*

If $r = 1$, and $\mathcal{T}_h$ satisfies Condition (ϵ, σ), then

$$\begin{aligned}&\|\nabla u - G_h u_h\| \\ &\lesssim \left(h \max\{h^{1/2}, \epsilon, h^{\sigma/2}\} + h^2 + h^{1+\frac{\beta-1}{2}}\right)(\|u\|_{3,\Omega} + \|u\|_{2,\Omega} + |u|_{2,\infty,\Omega}).\end{aligned}$$

If $r = 2$, and $\mathcal{T}_h$ is uniform or strongly regular, then

$$\|\nabla u - G_h u_h\| \lesssim \left(h^3 + h^{2+\frac{\beta-1}{2}}\right)(\|u\|_{4,\Omega} + \|u\|_{3,\Omega}).$$

If $r = 2$, and $\mathcal{T}_h$ satisfies Condition (ϵ, σ), then

$$\begin{aligned}&\|\nabla u - G_h u_h\| \\ &\lesssim \left(h^2 \max\{h^{1/2}, \epsilon, h^{\sigma/2}\} + h^3 + h^{2+\frac{\beta-1}{2}}\right)(\|u\|_{4,\Omega} + \|u\|_{3,\Omega} + |u|_{3,\infty,\Omega}).\end{aligned}$$

Consequently, it is now straightforward to prove asymptotic exactness of an error estimator based on the recovery operator G_h. We naturally define a global error estimator by

$$\Theta_h := \|G_h u_h - \nabla u_h\|_{L^2(\Omega)}. \tag{42}$$

And without loss of generality, the small quantity ϵ is assumed to be of $O(h^\alpha)$ with $\alpha > 0$. Then we get the following result parallel to Theorem 5.1 in [24].

Theorem 4.2. *Under the assumptions of Theorem 4.1, and if there exists a constant $C(u) > 0$ such that*

$$\|\nabla(u - u_h)\| \ge C(u) h^r, \quad r = 1, 2. \tag{43}$$

Then it holds

$$\left|\frac{\Theta_h}{\|\nabla(u - u_h)\|} - 1\right| \lesssim h^\rho, \quad \rho = \min\left\{\frac{1}{2}, \frac{\sigma}{2}, \alpha, \frac{\beta - 1}{2}\right\}. \tag{44}$$

Proof. Applying Theorem 4.1 and (43) results in

$$\left|\frac{\Theta_h}{\|\nabla(u - u_h)\|} - 1\right| \le \frac{\|\nabla u - G_h u_h\|}{\|\nabla(u - u_h)\|} \le \frac{h^{r+\rho}(\|u\|_{r+2,\Omega} + |u|_{r+1,\infty,\Omega})}{C(u) h^r} \lesssim h^\rho, \tag{45}$$

where $r = 1, 2$. ∎

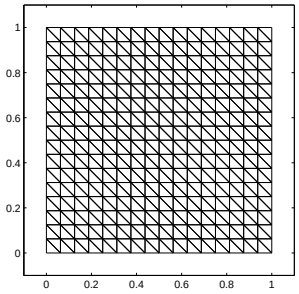

FIGURE 6. The regular pattern.

Remark 2. It is observed that the error estimator (42) based on the gradient recovery operator G_h is asymptotically exact under the triangulation $\mathcal{T}_h$ satisfying uniform, strongly regular, or *Condition* (ϵ, σ). Especially, *Condition* (ϵ, σ) is not restrictive in many cases. When some mildly structured grids are produced by any automatic mesh generators, they often satisfy this condition.

5. **Numerical results.** In this section we give the following cases with exact solutions to check the supconvergence of the OPSIPG method with the PPR technique for solving linear elliptic equations.

Let $\Omega = [0,1]^2$, $\partial\Omega = \Gamma_D$ and the variant coefficient $\alpha = 0$. Assume that $\mathbf{K}$ is an identity matrice, and the problem has the following exact solution:

$$\begin{aligned} &\text{Case1.} \quad u(x,y) = x(1-x)y(1-y); \\ &\text{Case2.} \quad u(x,y) = 2sin(\pi x)sin(\pi y). \end{aligned}$$

The source term function f and the (homogenous) boundary condition are given by the exact solution. The relative L^2-norm and H^1-seminorm errors are given by

$$\|e_h\| = \frac{\|u - u_h\|}{\|u\|}, \quad \|\nabla e_h\| = \frac{\|\nabla u - \nabla u_h\|}{\|\nabla u\|}.$$

An inner domain $\Omega_{\text{in}} = [0.1, 0.9]^2$ has been chosen for the following computation.

Under the regular pattern (see Figure 6 for the mesh used), Figures 8-9 compare the performance of the gradient recovery method implemented on the interior penalty discontinuous Galerkin method and the direct results from the interior penalty discontinuous Galerkin method. One may observe second-order convergent rates of the recovered gradient against approximately first-order convergent rates for the DG method without the use of the recovery technique. When the size of each patch is expanded to $4h$, Figures 10-11 show their superconvergence rates are preserved.

Under the chevron pattern (see Figure 7 for the mesh used), the recovery method for Case 1 performs well with a 2.03rd order convergent rate in the inner region as in Figure 12, while it also provides a superconvergent recovery of order 2.1 in the inner region in Figure 13 for Case 2. If the size of each patch is enlarged to $4h$, one can observe that they even have superconvergence property with order 2 in Figures 14-15. The numerical experiments demonstrated that the PPR-recovered gradient enjoys superconvergence.

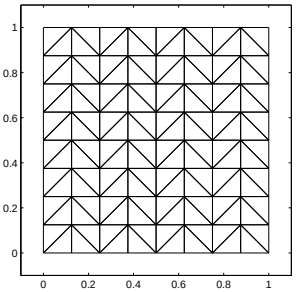

FIGURE 7. The chevron pattern.

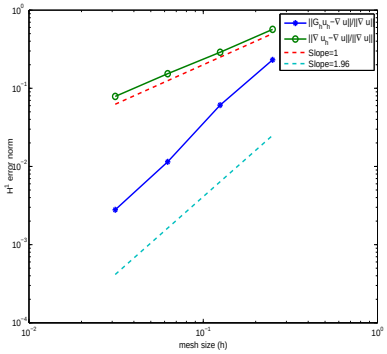

FIGURE 8. Linear element under the regular pattern for *Case 1*, Gradient Recovery Vs. the original H^1 seminorm errors.

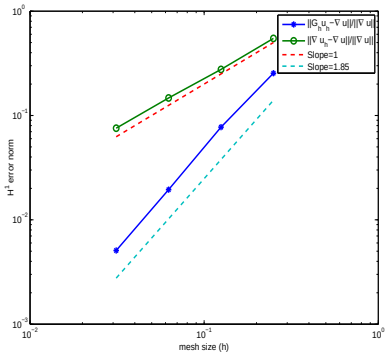

FIGURE 9. Linear element under the regular pattern for *Case 2*, Gradient Recovery Vs. the original H^1 seminorm errors.

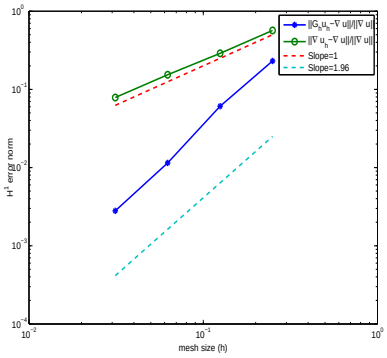

FIGURE 10. Linear element under the regular pattern with a larger patch of diameter $4h$ for *Case 1*, Gradient Recovery Vs. the original H^1 seminorm errors.

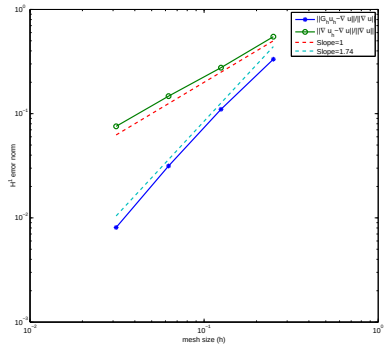

FIGURE 11. Linear element under the regular pattern with a larger patch of diameter $4h$ for *Case 2*, Gradient Recovery Vs. the original H^1 seminorm errors.

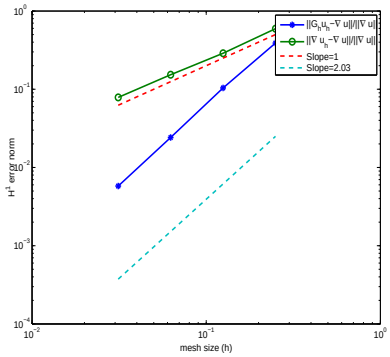

FIGURE 12. Linear element under the chevron pattern for *Case 1*, Gradient Recovery Vs. the original H^1 seminorm errors.

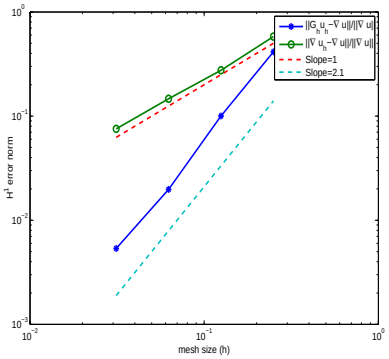

FIGURE 13. Linear element under the chevron pattern3 for *Case 2*, Gradient Recovery Vs. the original H^1 seminorm errors.

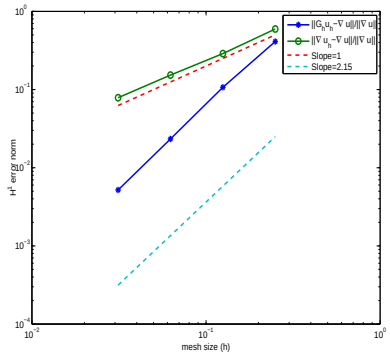

FIGURE 14. Linear element under the chevron pattern with a larger patch of diameter $4h$ for *Case 1*, Gradient Recovery Vs. the original H^1 seminorm errors.

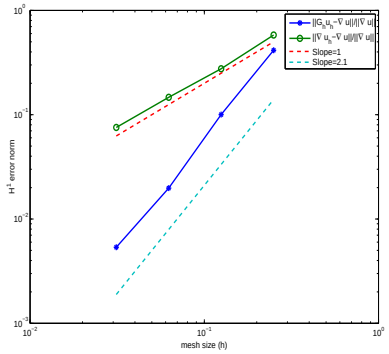

FIGURE 15. Linear element under the chevron pattern with a larger patch of diameter $4h$ for *Case 2*, Gradient Recovery Vs. the original H^1 seminorm errors.

For the quadratic element under the regular pattern, Figures 16-17 illustrate the superconvergence of the PPR in Cases 1 and 2, respectively. Analogously, the PPR for the quadratic element under the chevron pattern is superconvergent for the first two Cases in Figures 18-19. The gradient recovery seems better for the regular pattern than for the chevron pattern.

Case 3. Our last example is to solve a problem with singularity in the L-shaped domain $\Omega = (0,1)^2 \backslash [1/2,1)^2$ with $\mathbf{K} = \mathrm{I}_{2\times 2}$. Under a polar coordinate system (r,θ) with the origin $(\frac{1}{2},\frac{1}{2})$, the exact solution is

$$u(r) = r^{\frac{2}{3}} sin\Big(\frac{2\theta-\pi}{3}\Big), \quad \frac{\pi}{2} \le \theta \le 2\pi,$$

and the Dirichlet boundary condition is imposed.

Note that the solution in Case 3 has a corner singularity at the node $(1/2,1/2)$ with the reentrant corner of the interior angle $\frac{3\pi}{2}$. Therefore, the solution has the regularity $u \in H^{\frac{5}{3}-\tau}(\Omega)$, where τ is any positive number. In order to recover the

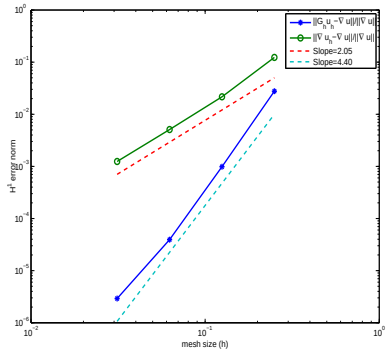

FIGURE 16. Quadratic element under the regular pattern for *Case 1*, Gradient Recovery Vs. the original H^1 seminorm errors.

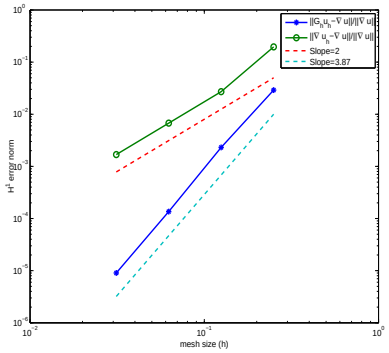

FIGURE 17. Quadratic element under the regular pattern for *Case 2*, Gradient Recovery Vs. the original H^1 seminorm errors.

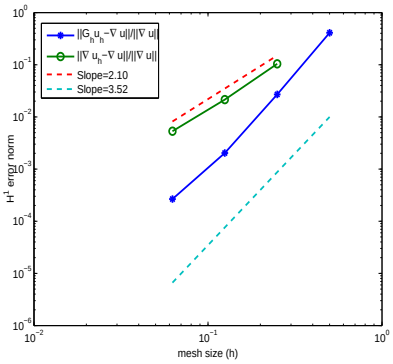

FIGURE 18. Quadratic element under the chevron pattern for *Case 1*, Gradient Recovery Vs. the original H^1 seminorm errors.

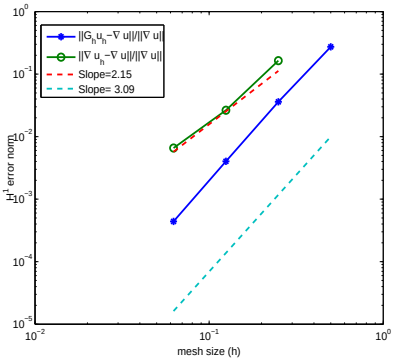

FIGURE 19. Quadratic element under the chevron pattern for *Case 2*, Gradient Recovery Vs. the original H^1 seminorm errors.

convergent rate obtained with the polynomial degrees, we need to locally refine the mesh around the origin. Locally refined meshes from a distmesh programme in [15] have been considered. The domain is decomposed into two parts: one is the interior subdomain $\Omega_a := [0.08, 0.92] \times [0.08, 0.42] \cup [0.08, 0.42] \times [0.42, 0.92]$, and the other one is the boundary layer $\Omega_b = \Omega \backslash \Omega_a$ with a width of 0.08. For the penalty term, we use superpenalization, and choose $\beta = 3$ and $\sigma_e = \frac{1}{19}$ on every edge. By the gradient recovery method based on a locally refined mesh in Figure 20, we define by the ratio

$$\frac{\|\Theta_h\|_{L^2(\Omega_a)}}{\|\nabla u - \nabla u_h\|_{L^2(\Omega_a)}} - 1 \approx O(N^{\sigma}).$$

It is observed in Figure 21 that $\|\nabla u - G_h u_h\|_{L^2(\Omega_a)}$ is superconvergent with order $O(N^{-1.46})$, and the term $\|G_h u_h - \nabla u_h\|_{L^2(\Omega_a)} / \|\nabla u - \nabla u_h\|_{L^2(\Omega_a)}$ approaches 1 at the rate of $O(N^{-2.19})$ in the interior subdomain. Due to the regularity of the exact

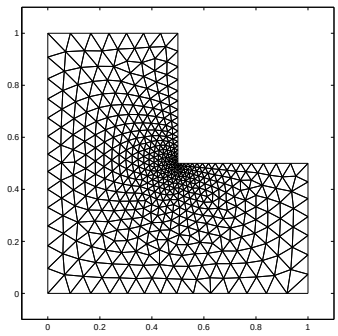

FIGURE 20. Linear element for a locally refined mesh used in *Case 3*.

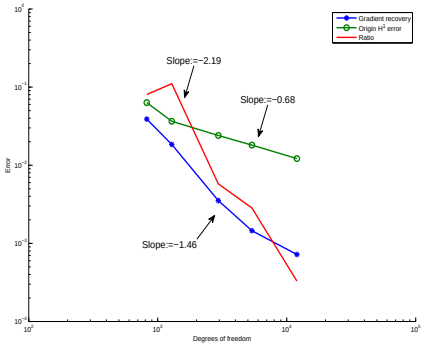

FIGURE 21. Linear element, absolute errors $\|\nabla u - G_h u_h\|_{L^2(\Omega_a)}$, $\|\nabla u - \nabla u_h\|_{L^2(\Omega_a)}$ and ratio Vs. N (the total number of degrees of freedom) for *Case 3*.

solution, we also find the errors in the energy norm on the discontinuous Galerkin solutions is up to order $O(N^{-2/3})$. It is observed that the polynomial preserving recovery technique for the OPSIPG method produces a superconvergent recovered gradient.

In summary, based on the OPSIPG method, the PPR produces superconvergent results for linear element under the regular pattern and under the chevron pattern; while for quadratic element, the PPR is superconvergent under both the regular and the chevron patterns.

REFERENCES

[1] M. Ainsworth and J. T. Oden, *A Posteriori Error Estimation in Finite Element Analysis*, Wiley Interscience, New York, 2000.

[2] D. N. Arnold, An interior penalty finite element method with discontinuous elements, *SIAM J. Numer. Anal.*, **19** (1982), 742–760.

[3] I. Babuška and W. C. Rheinboldt, A-Posteriori Error Estimates for the Finite Element Method, *Internat. J. Numer. Methods Engrg.*, **12** (1978), 1597–1615.

[4] I. Babuška and T. Strouboulis, *The Finite Element Method and Its Reliability*, Oxford University Press, London, 2001.

[5] R. E. Bank and A. Weiser, Some a posteriori error estimators for elliptic partial differential equations, *Math. Comp.*, **44** (1985), 283–301.

[6] C. Brenner, L. Owens and L.-Y. Sung, A weakly over-penalized symmetric interior penalty method, *Electron. Trans. Numer. Anal.*, **30** (2008), 107–127.

[7] S. C. Brenner, T. Gudi and L.-Y. Sung, A posteriori error control for a weakly over-penalized symmetric interior penalty method, *J. Sci. Comput.*, **40** (2009), 37–50.

[8] E. Burman and A. Ern, Continuous interior penalty hp-finite element methods for advection and advection-diffusion equations, *Math. Comp.*, **76** (2007), 1119–1140.

[9] P. G. Ciarlet, Basic error estimates for elliptic problems, in *Handbook of Numerical Analysis, Vol. II* (eds. P.G. Ciarlet and J.L. Lions), North-Holland, Amsterdam, (1991), 17–351.

[10] Y. Epshteyn and B. Rivière, Estimation of penalty parameters for symmetric interior penalty Galerkin methods, *J. Comput. Appl. Math.*, **206** (2007), 843–872.

[11] P. Grisvard, *Elliptic Problems in Nonsmooth Domains*, Monogr. Stud. Math. 24, Pitman (Advanced Publishing Program), Boston, MA, 1985.

[12] Y. Huang and J. Xu, Superconvergence of quadratic finite elements on mildly structured grids, *Math. Comp.*, **77** (2008), 1253–1268.

[13] A. Naga and Z. Zhang, The polynomial-preserving recovery for higher order finite element methods in 2D and 3D, *Discrete Continuous Dynam. Systems - B*, **5** (2005), 769–798.
[14] P. Oswald, On a BPX-preconditioner for P1 elements, *Computing*, **51** (1993), 125–133.
[15] P. O. Persson and G. Strang, A simple mesh generator in Matlab, *SIAM Rev.*, **46** (2004), 329–345.
[16] B. Rivière, *Discontinuous Galerkin Methods for Solving Elliptic and Parabolic Equations: Theory and Implementation*, SIAM, Philadelphia, PA, 2008.
[17] M. F. Wheeler, An elliptic collocation-finite element method with interior penalties, *SIAM J. Numer. Anal.*, **15** (1978), 152–161.
[18] Z. Zhang, Polynomial preserving gradient recovery and a posteriori estimate for bilinear element on irregular quadrilaterals, *Int. J. Num. Anal. Model.*, **1** (2004), 1–24.
[19] Z. Zhang and A. Naga, A new finite element gradient recovery method: Superconvergence property, *SIAM J. Sci. Comput.*, **26** (2005), 1192–1213.
[20] Z. Zhang and A. Naga, A posteriori error estimates based on polynomial preserving recovery, *SIAM J. Numer. Anal.*, **42** (2004), 1780–1800.
[21] Z. Zhang, Polynomial preserving recovery for meshes from Delaunay triangulation or with high aspect ratio, *Numer. Methods Partial Differential Equations*, **24** (2008), 960–971.
[22] O. C. Zienkiewicz and J. Z. Zhu, A simple error estimator and adaptive procedure for practical engineering analysis, *Internat. J. Numer. Methods Engrg.*, **24** (1987), 337–357.
[23] O. C. Zienkiewicz and J. Z. Zhu, The superconvergent patch recovery and a posteriori error estimates, Part 1: The recovery technique, *Internat. J. Numer. Methods Engrg.*, **33** (1992), 1331–1364.
[24] J. Xu and Z. Zhang, Analysis of recovery type a posteriori error estimators for mildly structured grids, *Math. Comp.*, **73** (2004), 1139–1152.

Received February 2014; revised January 2015.

E-mail address: song@lzu.edu.cn
E-mail address: zzhang@math.wayne.edu